Geophysical implications of a decentered inner core

Călin Vamoş*
"T. Popoviciu" Institute of Numerical Analysis, Romanian Academy, P.O. Box 68, 400110 Cluj-Napoca, Romania

Nicolae Suciu†
Department of Mathematics, Friedrich-Alexander University of Erlangen-Nuremberg, Cauerstr. 11, 91058 Erlangen, Germany

arXiv:1402.6494v1 [physics.geo-ph] 26 Feb 2014

In a first approximation, the Earth's interior has an isotropic structure with a spherical symmetry. Over the last decades the geophysical observations have revealed, at different spatial scales, the existence of several perturbations from this basic structure. In this paper we discuss the hemispheric perturbations induced to this basic structure if the inner core is displaced from the center of mass of the Earth. Using numerical simulations of the observed hemispheric asymmetry of the seismic waves traveling through the upper inner core, with faster arrival times and higher attenuation in the Eastern Hemisphere, we estimate that the present position of the inner core is shifted by tens of kilometers from the Earth's center eastward in the equatorial plane. If the only forces acting on the inner core were the gravitational forces, then its equilibrium position would be at the Earth's center and the estimated displacement would not be possible. We conjecture that, due to interactions with the flow and the magnetic field inside the outer core, the inner core is in a permanent chaotic motion. To support this hypothesis we analyze more than ten different geophysical phenomena consistent with an inner core motion dominated by time scales from hundreds to thousands of years.

I. INTRODUCTION

Situated at the Earth's center, surrounded by the fluid outer core (OC), the inner core (IC) is primarily composed of a solid iron and nickel alloy. For a long time after its discovery by Lehmann in 1936 [51], it was modeled as an ideal mathematical object: a rotational ellipsoid with a smooth surface and a homogeneous and isotropic internal structure. But over the last decades the quality and the amount of geophysical observations have increased so that the IC image has become more complex and even contradictory [21, 81]. In this paper we show that many of the disputed issues and unresolved difficulties related to the IC can be simultaneously simplified or even solved by the hypothesis of an eastward displacement of the IC by tens of kilometers from the Earth's center in the equatorial plane.

If the fluid in the OC is at rest, then the equilibrium position of the IC at the Earth's center of mass is imposed by its gravitational interaction with the rest of the Earth. A permanent shift from this static equilibrium position is possible only if other forces act on the IC. In Sect. II A, using the recent results of numerical simulations of the geomagnetic dynamo [6], we tentatively identify the perturbing forces with those describing the electromagnetic and hydrodynamic interactions of the IC with the asymmetric convective flow in the OC. Then in Sect. II B we propose the global forcing of a decentered IC as a source of the nonhydrostaticity of the Earth's shape. Finally, in Sect. II C we show that our hypothesis is supported by the long standing observational difficulties in measuring the effects of the translational oscillations of the IC about the static equilibrium position (the Slichter mode). In conclusion, we conjecture that the IC participates and interacts with the turbulent convective flow in the OC being driven into a chaotic motion with time scales similar to those of the secular variations of the geomagnetic field near the equator.

In the next three sections we leave aside the dynamic considerations and using recent seismic observations we obtain an estimation of the present position of the IC. In Sect. III we resume the results presented in [89] where we analyzed the isotropic hemispheric asymmetry at the top of the IC (ATIC) of the travel times of the PKIKP seismic waves which propagate through the layer of 100 km thick below the inner core boundary (ICB). Using ray theory we numerically computed the PKIKP travel times for an eccentric position of the IC (Appendix B) and we showed that the displacement of the IC toward 110° E in the equatorial plane by tens of kilometers from the Earth's center can explain both the values and the geographical distribution of the differential travel times of the PKiKP-PKIKP phases. By means of the same numerical model, in Sect. IV we show that the decentering of the IC also explains the hemispheric asymmetry of the attenuation within the same region of the IC. So both hemispheric seismic asymmetries at the top of the IC are simultaneously explained by geometrical considerations related to the displacement of the IC, without disturbing the symmetry of the internal structure of the IC.

The differential travel times used to analyze the ATIC are not affected by the large perturbations due mainly to mantle heterogeneity. In Sect. V we use the absolute travel times of the seismic waves reflected at the ICB under small angles and we document for the first time the likely existence of an hemispheric asymmetry which could be related to a decentered position of the IC. The result is not as rigorous as those obtained in the previous two sections because we do not eliminate the perturba-

* cvamos@ictp.acad.ro
† suciu@math.fau.de

tions due to mantle heterogeneity, positioning errors of the earthquake epicenters, or misidentification of the precritical PKiKP phase.

An eccentric IC should influence many geophysical phenomena which can be used as additional means to substantiate our hypothesis. Section VI contains qualitative analyses of some of these geophysical phenomena: the anomalous layer above the ICB; the differential rotation of the IC with respect to the mantle; the large-scale anomalies of the geoid; the hemispherical pattern in the anisotropy level of the seismic waves velocity inside the IC.

The hypothesis of an IC displaced by 100 km from the Earth's center was formulated by Barta since the 1970's based on the distributions of the large-scale anomalies of the geoid [7–9]. Other two more qualitative justifications of this hypothesis were formulated in the same period and are briefly presented in Appendix A. The decentering of the IC has also recently been derived as a consequence of the theory of translational convection inside the IC [1, 2], but the supposed displacement is of only 100 m, so that the IC remains in mechanical equilibrium (see Appendix A).

II. DYNAMICS OF A DECENTERED IC

The main obstacle to accept the possibility that the IC could be decentered by tens of kilometers is the identification of forces large enough to displace the IC from its static equilibrium position. In this section we explore some of the evidences supporting the existence of such forces and of their dynamical effects on the IC. The ability of the IC to be driven by the flow inside the OC has to be tested through direct numerical simulations.

A. Flow and geomagnetic field inside the OC

Mechanical and electromagnetic interactions between the IC and OC, together with the very presence of the IC, affect the geometry of the flow inside the fluid OC and the geomagnetic field. The decentering of the IC is an additional geometrical and mechanical forcing which influences the structure of the magnetic field. In the following we try to identify the features of the geomagnetic field which support the existence of such an asymmetric forcing inside the Earth. First we briefly present the basic structure of the geomagnetic field which can be explained by symmetric numerical geodynamo models.

The radial components of the geomagnetic field at the core-mantle boundary (CMB) can be computed from the magnetic field at Earth's surface assuming that no sources exist between the Earths surface and the CMB [64]. The imaginary cylinder coaxial with Earth's rotation axis and tangent to the IC at the equator, known as the tangent cylinder, separates two regions of the OC in which the fluid flow and the resulting magnetic field are quite different. The most prominent features in the maps of the vertical field at the CMB are the high intensity flux lobes under Arctic Canada, Siberia, and under the eastern and western edges of Antarctica [45]. These lobes give the predominantly dipole field structure observed at the surface which has remained approximately stationary over the past four centuries. The flow near the top of OC derived from the magnetic field at the CMB using a kinematic model also contains polar vortices [37].

There are many numerical dynamo models which can explain the main properties of the geomagnetic field [16]. For example, numerical simulations generate weaker field inside the tangent cylinder, strong normal polarity flux lobes close to the tangent cylinder, and pairwise inverse field patches around the equator. An outstanding difficulty for standard models has been how to reproduce the westward drift of low-latitude magnetic flux patches at the CMB. At Earth's surface they correspond to field variations with timescales shorter than 400 years, between 20° N and 20° S with speed of approximately 17 km/yr westward [45].

A simple geometrical reasoning shows that the IC could be the cause of this phenomenon. If the IC is displaced in the equatorial plane, then its mechanical and thermal forcing on the OC is concentrated between two planes parallel with the equator and tangent to the IC, i.e., within a spherical segment with the height equal with the IC diameter of 2442 km. This height differs only by a few percents from the width at the CMB of the westward-moving wave-like patterns equal to $2R_{\rm OC}\sin 20^\circ = 2380\,\text{km}$, where $R_{\rm OC} = 3480\,\text{km}$ is the OC radius.

A more elaborate justification is provided by the first successful numerical simulation of the westward drift of the magnetic field, obtained by means of a heterogeneous thermodynamical boundary condition at both the ICB and CMB and a gravitational coupling of the IC with the mantle [6]. This dynamo model produces magnetic variations dominated by intense, westward-drifting, equatorial flux patches under the Atlantic hemisphere. The maximum of the magnetic power moving in the longitudinal direction is reached at the Equator, with a maximum speed of 14 km/yr, comparable to that observed of 17 km/yr.

The numerical simulated convection in the OC is dominated by the mass flux at the ICB modeled by a longitudinal hemispherical heterogeneity, maximal at the longitude of 90 °E. This asymmetric forcing could be caused by the displacement of the IC in the direction of the maximum mass flux. Because of the smaller distance between the ICB and the CMB, in this direction the temperature gradient should be larger and the mass flux should be increased. The gravitational coupling between the IC and the mantle could be a secondary effect of the displacement of the IC.

An important result obtained by this numerical simulation related to the IC dynamics is the strong large-scale asymmetry of the flow and of the magnetic field inside

the OC. The rotational turbulent hydrodynamic flow in the OC can become asymmetric at planetary scale, firstly by interaction with the IC and secondly by the heterogeneous forcing at the CMB. The asymmetry of the flow and of the magnetic field at the CMB is also supported by the observation data [29, 38]. Such a complex flow could generate significant viscous and magnetic forces on the IC [3, 13, 14] and could maintain it in a permanent chaotic motion. These forces should increase when the nondimensional parameters characterizing the numerical simulations will further approach the real values for the deep Earth. The time scales characteristic to the IC motion have to be larger than several decades which is the time scale associated to the westward drift of the geomagnetic field.

The relation between the direction of the highest light-element mass flux at the ICB and the offset of the magnetic dipole from the Earth's center [65] also supports our hypothesis of a decentered IC. The drastic change in the dipole position from the Western to the Eastern Hemisphere during the last 10000 years could be explained by a complete reversal of the direction of the faster IC growth, which in turn could result from intermittent IC rotation [65]. A simpler explanation might be the movement of the IC from the Western to Eastern Hemisphere, which reverses the direction of the maximum mass flux associated with the hemispheric asymmetry of the magnetic field [6]. This provides an upper limit of several thousands of years for the time scales of the IC motion. In addition, the intricate trajectory of the dipole is an indication that the motion of the IC is likely chaotic.

B. The variation of the Earth's rotation

The dynamic forcing of a decentered IC should be transmitted to the entire Earth. Here we briefly discuss its influence on the rotational motion of the Earth and on the nonhydrostaticity of the Earth's shape. Variations of the Earth rotation manifest as variations in direction of Earth's rotation axis as well as variations in the angular speed, i.e., variations in the length of day (LOD). Precession of an axis is the mean, smoothly varying part of the motion of the axis relative to the direction of fixed stars while nutation is the oscillatory part of this motion [23]. The motion of the instantaneous rotation axis with respect to the figure of the Earth is known as the Earth wobble.

The influence of the IC on the wobble and nutation of the Earth can be determined from a three-layer model of a deformable Earth [23]. The results of the numerical model are a set of optimized values for the Earth parameters derived from the "best fit" with observational data. We are first interested in the inference that the ellipticity of the core has to be about 5% higher than its value for the hydrostatic equilibrium Earth model [35]. The nonhydrostatic excess of the ellipticity corresponds to a difference of approximately 400 m between the equatorial and polar radii of the CMB.

This nonhydrostaticity has been attributed to the mantle convection [23]. Another cause could be that the IC displacement perturbs not only the OC, but also the mantle, mainly in the equatorial region. Our estimations indicate a displacement of the IC from the Earth's center in the equatorial plane of tens of kilometers (Sects. III, IV, and V). This is almost two orders of magnitude larger than the displacement deduced from mechanical and thermal equilibrium conditions [1]. Such a large difference implies a nonhydrostatic evolution of the IC and, implicitly, of the rest of the Earth.

Another phenomenon possibly influenced by the IC displacement is the Makowitz wobble, which is the motion of the pole with respect to the Earth's crust and mantle including a quasiperiodic component with a period of approximately 24 years superimposed on a linear drift [32]. The cause of the decadal-scale polar motion variations is currently unknown. It was found that the main excitation source of the variations cannot be the redistribution of mass within the atmosphere and oceans or the core-mantle coupling. The most probable source is the IC, but the suggestion that irregular motion of a tilted oblate IC may excite the Makowitz wobble was proved to be unlikely. An eccentric IC could have the additional independent parameters needed to explain this wobble.

The rotation period of the Earth is not uniform, but varies on time scales from days to millennia [32]. The tidal drag of the Moon and Sun on the rotating Earth produces a secular slowing down of the rotation. The angular momentum variations of the atmospheric and oceanic global circulation explain most of the observed LOD variation at yearly and subyearly timescales. In addition, there are variations over several decades related to the angular momentum in the core which are well modeled for the past century [44]. Prior to this period the results are poorer, especially because of a phase shift, but the general pattern is still remarkable. The supposed displacement of the IC would affect the global angular momentum of the Earth and could be an explanation of the phase shift. Then the dominant time scales of the IC movement could be at least several hundreds of years.

C. Translational oscillations of the IC

An equilibrium position of the IC at the Earth's center of mass is primarily determined by the gravitational field. The gravitational restoring force is proportional with the displacement of the IC from the Earth's center and with the density difference between the IC and the surrounding OC. A large earthquake or a large meteorite impact could initiate harmonic oscillations about this equilibrium position. If ω_0 is the angular frequency for oscillations parallel to the Earth's rotation axis, then the oscillations in the equatorial plane have two eigen-

values $\omega_0 \pm \Omega$, where Ω is the Earth's angular velocity. The three modes of translational oscillations are known as Slichter modes after the researcher who first predicted them [77].

The frequencies of the Slichter modes are influenced by many factors: the stratification of the fluid in the OC, the elastic properties of the IC and OC, the viscosity of the fluid in the OC, the magnetic perturbations near the ICB, the mushy structure of the ICB, etc. [74]. Depending on the approximations used to model these factors, the theoretically computed periods vary from 4 to 8 h according to different authors. But this mode has never been clearly identified from observational data and it is still a subject of interest and debate. The Slichter mode was not observed even in the records obtained after the huge Sumatra-Andaman earthquake of December 2004 [63, 75].

It is obvious that the inability to detect the Slichter mode could be due to the insufficient sensitivity of the currently available superconducting gravimeters. However, taking into account that all the other normal modes of the Earth have been identified from the seismic data, it is possible that the translational oscillations simply do not take place because the gravitational restoring force is not the only force acting on the IC. If, as we have conjectured in Sect. II A, the IC is in a chaotic motion correlated to the turbulent flow in OC, then the momentum transferred by an earthquake would not cause the oscillation of the IC, but it would determine only an additional displacement. Hence the difficulty to determine the Slichter mode could be an indication that the IC is not in an equilibrium position at the Earth's center.

III. RESIDUALS OF THE PKiKP-PKIKP DIFFERENTIAL TRAVEL TIME

In this section we begin to determine the present position of the IC using seismic data. One of the best documented seismic hemispheric asymmetry is the isotropic asymmetry at the top of the inner core (ATIC) characterized by an Eastern Hemisphere with faster arrival times of the P-waves and a Western Hemisphere with slower arrivals [15, 30, 61, 67, 94–96]. ATIC has been mainly documented by the residuals of the differential travel time of the PKIKP and PKiKP seismic phases [61, 92–96]. They both travel through almost the same regions of the crust, mantle, and OC. After that, the PKiKP phase reflects off the ICB, while the PKIKP phase refracts twice on ICB propagating inside the IC.

We denote by Δt the observed differential travel time obtained by subtracting the travel time of the PKIKP phase from the travel time of the PKiKP phase with the same focus and exit point. It differs from the differential travel time Δt_0 computed for a centered IC with the velocity profile given by a one-dimensional reference seismic model. The observational data show that the residuals $\Delta t - \Delta t_0$ are positive in the Eastern Hemisphere and negative in the Western Hemisphere [61, 92, 94–96]. An important constraint for the models proposed to explain this hemispheric dichotomy is the sharpness of the boundaries separating the regions with positive and negative residuals [92, 93].

All existing explanations assume the center of the IC fixed at the center of the Earth and interpret the observed anomaly of the travel time residuals in terms of a longitudinal anomaly of the seismic wave velocity (e.g. [93]). Greater (smaller) seismic wave velocity at the top of the IC in the Eastern (Western) Hemisphere, with respect to 1D reference models, are explained by a hemispheric variation of the material properties at the top of the IC [1, 18, 61, 92–96]. There are two competing approaches to explain such an IC velocity asymmetry. The first one assumes different cooling rates in the Eastern and Western Hemispheres due to thermochemical coupling with the mantle [3, 84, 85], causing a faster solidification rate of the Eastern Hemisphere. Different textures of the IC material resulted from this process may explain the hemispherical pattern of the seismic velocity [17]. Alternatively, another approach proposes a self-sustained eastward translation of the IC as a result of crystallization in the Western Hemisphere and melting in the Eastern Hemisphere, followed by the west-east increase of the iron grain-size which could produce the velocity anomaly explaining the ATIC [1, 58]. Even whether these models explain the travel time anomaly, neither of them is fully consistent with the observed sharpness of the hemispheric boundaries [2, 93].

Using the numerical simulation presented in Appendix B we show that the ATIC can be explained by the displacement of the IC in the equatorial plane toward east by tens of kilometers from the Earth's center, without modifying the spherical symmetry in the upper IC. We denote by $\mathrm{PKIKP_{dec}}$ and $\mathrm{PKiKP_{dec}}$ the paths modified by the decentered IC. Unlike the paths for the centered IC, their propagation plane changes at reflection or refraction on ICB. Only when the seismic ray propagates in a plane containing both the center of the IC and of the Earth, the propagation plane does not change. A clear east-west asymmetry is obvious in Fig. 1 for such seismic rays having the same initial incidence angle, i.e., being identical until the incidence with the ICB.

From the differential times computed in Appendix B we determine the residuals shown in Fig. 2 for the seismic rays in the Eastern Hemisphere plotted in Fig. 1. They are quantitatively comparable with those observed [61, 92, 94–96] showing that displacements of the IC over distances up to 100 km can explain the travel time anomaly. With the increase of the turning point depth (epicentral distance) the positive residuals in the Eastern Hemisphere increase because the length of the path inside the IC increases (Fig. 9a).

In order to ascertain if a decentered IC can explain ATIC, we compare the longitudinal repartition of the residuals obtained by numerical simulations with those reported in [92, Fig. 3a] and in [93, Fig. 3b], the most

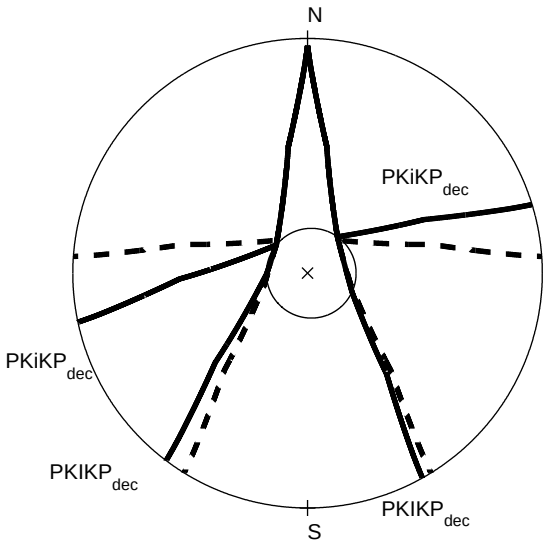

FIG. 1. The paths of the $PKIKP_{dec}$ and $PKiKP_{dec}$ rays (thick continuous lines) when the IC (the small circle) is displaced by 100 km from the Earth's center in the equatorial plane toward east. The epicenter is at the North Pole, the propagation plane of the seismic rays contains the centers of both Earth and decentered IC and, in this case, they are not modified by refraction or reflection on ICB. The dashed lines represent the paths of the same phases for the centered IC.

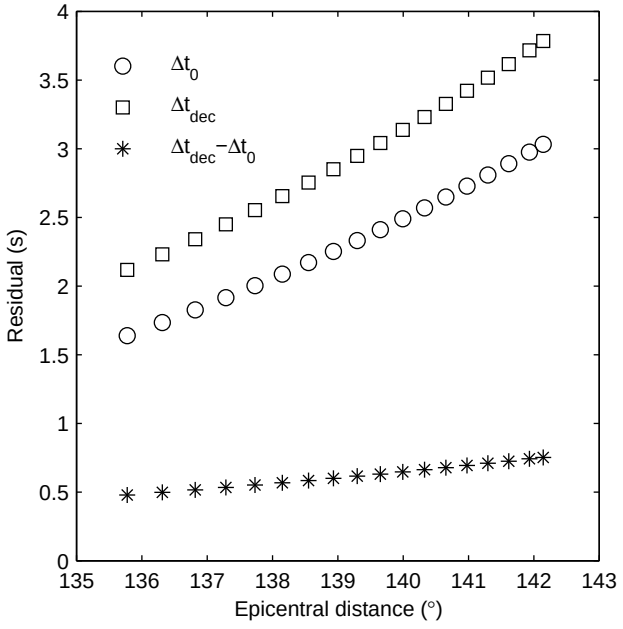

FIG. 2. Numerically computed residuals for a decentered IC. The differential travel times Δt_{dec} are computed for the $PKIKP_{dec}$ seismic rays in the Eastern Hemisphere plotted in Fig. 1.

extensive and accurate PKiKP-PKIKP studies to date. For a given position of the IC, we compute the residuals for earthquakes evenly distributed on the Earth's surface and seismic rays uniformly distributed around the focus (see Appendix B). For each seismic ray we choose the incidence angle so that the corresponding turning point is at 39 km below ICB, the minimum depth below ICB of the available observational data (see [92, Fig. 3a]).

Figure 3 shows the longitudinal distribution of the residuals when the IC is displaced by 100 km toward 90° E longitude. If the displacement is in the equatorial plane, then the positive residuals are confined within the Eastern Hemisphere and the negative ones within the Western Hemisphere (Fig. 3a). If the IC is displaced outside the equatorial plane, the separation of the positive and negative residuals is not so definite (Fig. 3b). In the observational data, the positive and negative residuals are sharply separated [92, 93] indicating that the displacement of the IC is in the equatorial plane (Fig. 3a). The observed boundary between the positive and negative residuals is shifted toward east by approximately 20° with respect to the boundary between the Eastern and Western Hemispheres. The numerically simulated boundary rotates with the angle equal with the difference between the longitude of the IC center and the 90° E longitude. All these indicate a displacement of the IC by tens of kilometers in equatorial plane toward 110° E longitude.

The theoretical residuals generated by a decentred IC have a cylindrical symmetry about the direction of the IC displacement. This distribution is consistent with the eyeball-shaped positive anomaly at low- and mid-latitude of the compressional velocity derived for a centered IC model from seismical observations [87]. The anomaly is centered on 90° E longitude on the equator, i.e., very close to the direction of the IC displacement estimated above. The theoretical distribution of the residuals also agrees with the lack of the hemispheric asymmetry at the south pole of the IC [62].

When the results of the numerical simulations are compared with observational data we have to take into account the simplifying hypotheses of the numerical simulation as well as the observational errors. For instance, we have used the velocities of the ak135 model obtained under the hypothesis that the IC is centered. But the observational differential travel times PKiKP-PKIKP are spread around the mean values of the ak135 model by about 0.5 s [49], which is comparable with the values associated with ATIC [92]. That is why the exact longitude separating the positive and negative observed residuals and its variation with the turning point depth of the seismic rays cannot be determined precisely. The observation data suggest an eastward shift of the hemisphere boundary with increasing depth [92], while our numerical simulations have shown that it does not vary with the depth.

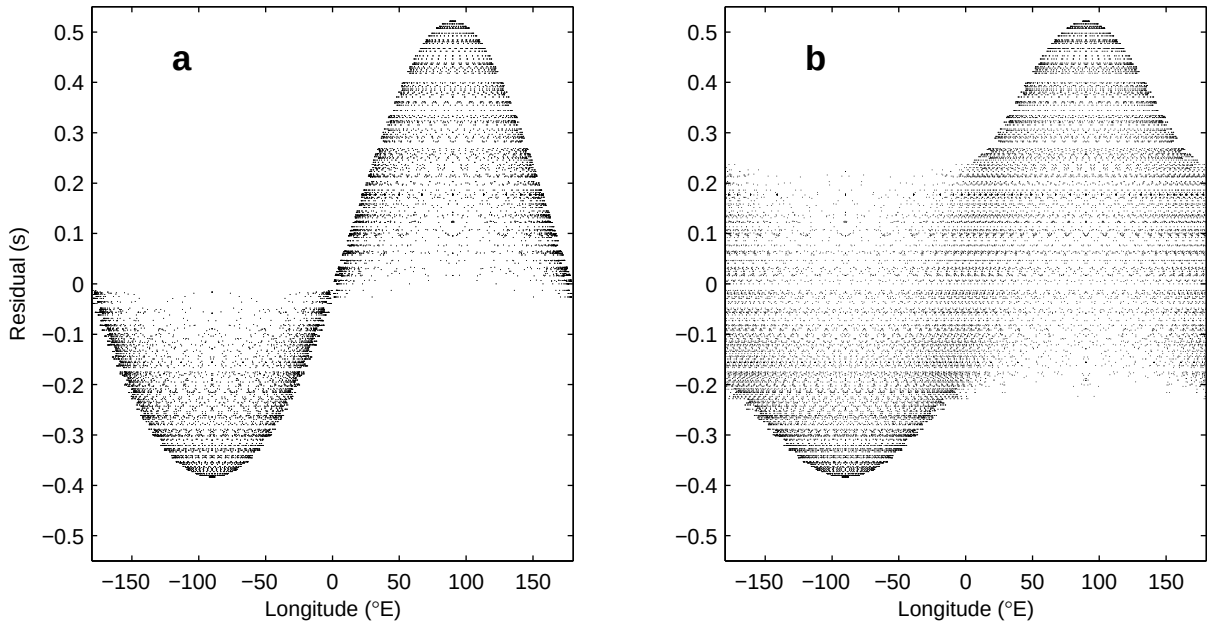

FIG. 3. Longitudinal distribution of the ATIC residuals obtained by numerical simulation. The IC is displaced by 100 km toward 90° E longitude in the equatorial plane (a) and along a direction making an angle of 30° with the equatorial plane (b). The abscissa represents the longitude of the turning point of the $\mathrm{PKIKP_{dec}}$ ray.

IV. HEMISPHERIC ASYMMETRY OF THE ATTENUATION IN THE UPPER IC

There are other seismic phenomena with east-west asymmetry, although without a complete observational description of their longitudinal variation, which may be explained by a decentered IC. For instance, ATIC is associated to a hemispheric asymmetry of the seismic waves attenuation [15, 40, 53, 66, 81, 94, 96] which seems to be confined to the uppermost IC [53, 81]. Existing explanations of the attenuation asymmetry require a trade-off between attenuation and velocity structures in the IC and velocity structure at the bottom of OC [94, 96]. Explanations of the hemispheric asymmetric attenuation are currently based on the specific texture of the uppermost IC [17] or on the assumption that a mushy zone exists at ICB [15].

If the IC is decentered, the $\mathrm{PKIKP_{dec}}$ phase propagates in the Eastern Hemisphere over a longer distance inside the IC (segment CD in Fig. 9a) than in the Western Hemisphere. Since the quality factor Q is two orders of magnitude larger in the OC than in the IC [49], the attenuation Q^{-1} in the Eastern Hemisphere is larger than in the Western Hemisphere. Hence the different lengths of the $\mathrm{PKIKP_{dec}}$ paths in Eastern and Western Hemispheres of the decentered IC explain not only the hemispherical asymmetry travel time residuals (Sect. III), but also the hemispheric asymmetry of the attenuation.

The quality factor Q at the top of the IC is determined by

$$\frac{A_{\mathrm{I}}}{A_{\mathrm{i}}} = exp\left\{-\frac{\pi f t}{Q}\right\},$$

where A_{I} and A_{i} are the amplitudes of the PKIKP and PKiKP phases at the common emerging point, f is the frequency and t is the travel time of PKIKP phase inside the IC [15]. The quantities A_{I}, A_{i}, and t are derived from measurements and the above relation is used to compute the quality factor Q.

The seismical observations show that the ratio $A_{\mathrm{I}}/A_{\mathrm{i}}$ depends not only on the epicentral distance Δ, but also on the geographic location. If one considers that the IC is centered, then the travel time inside the IC depends only on the epicentral distance $t_{\mathrm{cen}}(\Delta)$. In this case, the geographical variations of $A_{\mathrm{I}}/A_{\mathrm{i}}$ are possible only if the material properties vary inside the IC and the quality factor depends, besides the epicentral distance, also on the longitude and latitude of the turning point H, $Q_{\mathrm{cen}}(\Delta; \lambda_H, \phi_H)$. The quality factor Q_{cen} computed for a centered IC takes larger values in the Western Hemisphere than in the Eastern Hemisphere, the difference being larger at smaller epicentral distances [15, Fig. 5b].

In the following, we show how a displacement over 100 km of the IC in the equatorial plane can explain the seismical observations, without the need to modify the quality factor inside the IC. Using the numerical model presented in Appendix B, we compute the travel time of the PKIKP phase in a decentered IC, $t_{\mathrm{dec}}(\Delta; \lambda_H, \phi_H)$, which is a function of the longitude and latitude of the

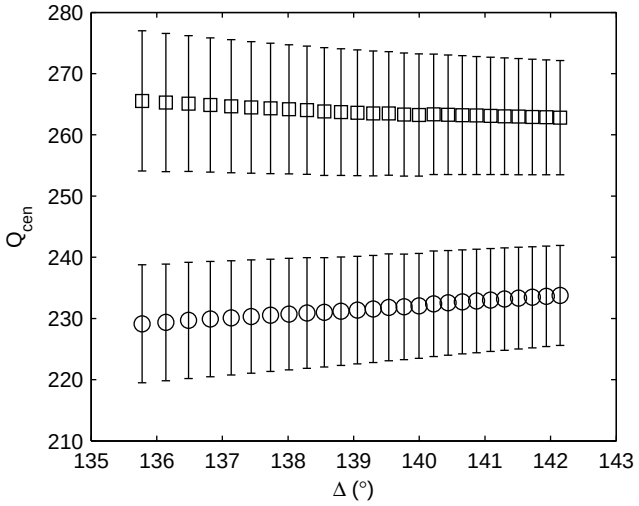

FIG. 4. Attenuation for a decentered IC. Average and standard deviation over the Eastern (circle markers) and Western (square markers) Hemispheres of the simulated quality factor $Q_{\rm cen}$ as a function of the epicentral distance.

turning point H. We describe the attenuation at the top of the IC by means of a constant quality factor $\overline{Q} = 247$ [15]. Then the two models of attenuation are related by the relation

$$\frac{t_{\rm cen}(\Delta)}{Q_{\rm cen}(\Delta;\lambda_H,\phi_H)} = \frac{t_{\rm dec}(\Delta;\lambda_H,\phi_H)}{\overline{Q}}.$$

If our hypothesis is correct, then the quantity $Q_{\rm cen}$ computed from this formula should be identical with that derived directly from observational data.

We have computed the mean and the standard deviation of $Q_{\rm cen}$ over all possible geographical positions (angles λ_H and ϕ_H), separately for east longitudes ($\lambda_H > 0$) and west longitudes ($\lambda_H < 0$). The numerical results presented in Fig. 4 show a good resemblance with the observational results (see [15, Fig. 5b]). The distance between the two branches of the graph decreases when the epicentral distance increases in the same way as for the observed data, although they do not intersect at epicentral distances greater than 140°. Also the observed differences for epicentral distances smaller than 140° are several times greater than those numerically computed.

V. HEMISPHERIC ASYMMETRY OF THE PRECRITICAL PKiKP TRAVEL TIME

A displacement of the IC should give rise to other hemispheric asymmetries of the seismic phases propagating through the IC. Unfortunately, due to the inhomogeneities of the Earth's interior, the absolute travel times for such seismic rays reaching the ICB are difficult to be determined and then the geographical repartition of the characteristics of the seismic waves is highly uncertain. The largest changes of the arrival times induced by the position of the ICB occur for the seismic rays reflected under small angles (near-normal PKiKP phase). Identification of such perturbations in seismic observations encounters two major difficulties.

First, in accordance with recent studies, the surface of the ICB has a rough topography [50] with height variations larger than 10 km which produce local fluctuations of several seconds of the near-normal PKiKP travel times [20]. Thus a displacement of the entire IC over a distance of the same order of magnitude is hidden by the local fluctuations and a large enough sample of data is needed to assure a significant statistical analysis. The second problem is related to the difficulty to identify the near-normal PKiKP phase from seismic observations [50, 76]. If the IC is decentered, then the identification is even harder because the arrival times can become quite different from those computed by a reference Earth model with spherical symmetry, which are used in phase identification procedures [28, 69, 76]. For instance, a 10 km displacement of the IC, which is comparable to the height of the ICB irregularities, causes a variation up to 2 s of the arrival times of the near-normal PKiKP waves. Therefore we expect that the near-normal PKiKP rays with the largest residuals are most probably misidentified.

Rather than relying on particular events with well identified and analyzed PKiKP phases, as for instance in [46, 47, 50, 71], we consider global data and follow a statistical approach. We use validated ISC data [39] to assemble a large enough sample which allows us to draw significant statistical conclusions. We downloaded information for all phases identified by ISC as PKiKP, irrespective of how they were initially reported. While before 2006 the reported PKiKP phases were generally not confirmed by the ISC analysts, since 2006 they identified the PKiKP phase and computed arrival times residuals with respect to the ak135 velocity model (D. A. Storchak, private communication, 2013). For our purpose, we select data with $\Delta < 90°$, which cover the whole range of precritical PKiKP and most of the transparent zone [47, 50].

From the validated data set 2006-2010 we have obtained a sample of 2042 residuals of the precritical PKiKP phase, plotted in Fig. 5 as function of the longitude of the bouncing points on the ICB. The residuals show large fluctuations similar to those reported in other recent studies on PKiKP phase [20, 50]. They have a negative mean of -0.745 s, with a standard deviation of 1.446 s and a standard error of the mean of 0.032 s (estimated by standard deviation divided by the square root of number of observations), in agreement with previous results obtained from smaller data sets [50]. Removal of the outliers from the data sample has insignificant influence on the statistical results derived in the following.

The sample of 2042 residuals contains 1669 observations with the bouncing point in the Eastern Hemisphere and only 373 observations in the Western Hemisphere. In the Eastern Hemisphere the mean of the residuals is

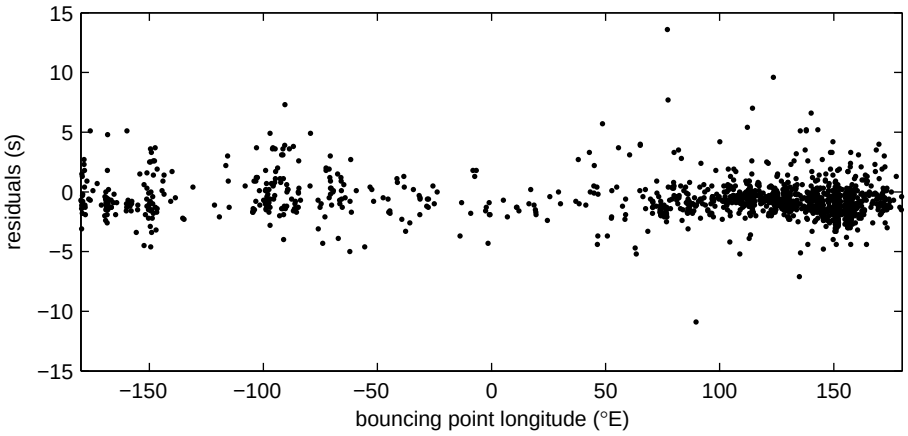

FIG. 5. Arrival time residuals with respect to the reference model ak135 of the PKiKP phase, recorded at epicentral distances smaller than 90°, as a function of the longitude of the bouncing points at the ICB.

-0.838 s, with standard deviation of 1.361 s and standard error of the mean of 0.033 s, while in the Western Hemisphere the mean residual is -0.328 s, with standard deviation of 1.720 s and standard error of the mean of 0.089 s. Thus, the data set shows a difference of 0.510 s between the mean precritical PKiKP residuals in the Western and Eastern Hemispheres, with a standard error of 0.095 s (computed considering that the two subsets of seismic events are independent). The west-est discrepancy of the mean residuals, with faster precritical PKiKP arrivals in the Eastern Hemisphere, indicates a global asymmetry not yet reported in the literature.

We assume that the maximum hemispheric asymmetry lies in the equatorial plane, as we already found in the previous sections. We search for a partition of the Earth into two disjoint hemispheres which yields the maximum difference of the hemispheric averages of the precritical PKiKP residuals. We denote by $\lambda_E \in [0°, 180°]$ the eastern longitude of the middle of the hemisphere H_E containing the greater part of the geographic Eastern Hemisphere. (We adopt the usual convention that eastern longitudes are positive, while western ones are negative.) Hence, the hemisphere H_E is defined by the longitudes $\lambda \in [\lambda_E - 90°, \lambda_E + 90°]$ if $\lambda_E \leq 90°$ and $\lambda \in [\lambda_E - 90°, 180°] \cup [-180°, \lambda_E - 270°]$ if $\lambda_E \geq 90°$. We denote by H_W the complement of H_E containing mostly western longitudes centered on the longitude $\lambda_W = \lambda_E - 180° < 0$. Figure 6 shows the mean residuals and the standard errors of the mean for PKiKP rays with bouncing points in the two hemispheres as a function of λ_E. For $70° \leq \lambda_E \leq 170°$ the mean residuals in the H_E hemisphere are smaller than in the H_W hemisphere by a quantity several times larger than the standard errors of the mean. The largest difference, equal to 0.55 s, is obtained for $\lambda_E = 140°$. For a wave velocity of about 10 km/s, this difference corresponds to a mean difference of 5.5 km between the paths of the PKiKP rays in the two hemispheres. Hence, the H_E hemisphere of the ICB centered on $\lambda_E = 140°$ is on average closer by 2.7 km to the Earth's surface than the corresponding H_W hemisphere.

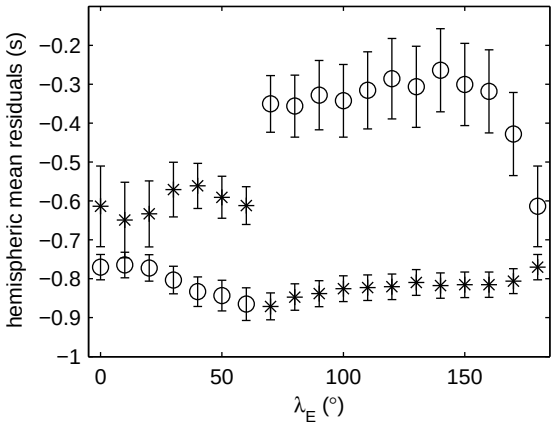

FIG. 6. Residuals averaged over the H_E hemisphere (asterisks) and over the H_W hemisphere (circles) as a function of longitude λ_E of the middle of H_E. Error bars represent standard errors of the mean.

In Fig. 6 our attention is drawn by the sudden reversal of the sign of the mean residuals when passing from $\lambda_E = 60°$ to $\lambda_E = 70°$. The jump occurs when the plane separating the two hemispheres rotates by 10° and the residuals with bouncing point longitude between 150°E and 160°E move from the H_W hemisphere to the H_E hemisphere. There are 589 such observations, i.e., 29% from the total number of observations (see Fig. 5). The sign reversal shows that these data are responsible for two thirds of the maximum difference of the mean residual obtained for $\lambda_E = 140°$. The remaining one third is due to the other residuals in the H_E hemisphere.

In order to confirm the existence of this new hemispherical seismic asymmetry, additional work is needed. The influence of the site effects, the near source hetero-

geneity, and the long wavelength mantle heterogeneities should be computed and subtracted for each travel time. Also the PKiKP phases reported by ISC should be individually verified and validated. However, all these perturbing effects are likely uncorrelated with the seismic events and they might have been significantly reduced by the statistical processing of the 2042 observations. If confirmed, this asymmetry is an indication that the value of 2.7 km should be an inferior limit for the IC displacement.

VI. OTHER GEOPHYSICAL IMPLICATIONS OF A DECENTERED IC

There are many geophysical phenomena containing qualitative and quantitative information regarding the position and the motion of the IC which could support the hypothesis of a decentered IC. For example, the bifurcation of the PKP phases occurring at smaller epicentral distance in the Eastern than in the Western Hemisphere [95, 96]. Also, the observation that travel time residuals of the PKiKP with respect to the $PKPB_{diff}$ phase, diffracted through the middle of the OC, are smaller by about 0.9 s in the Eastern Hemisphere than in the Western Hemisphere [95] is consistent with the PKiKP travel time hemispheric asymmetry presented in Sect. V and can be explained as well by the eccentric position of the IC.

Many of these geophysical phenomena with different types of asymmetries are related to the structure and evolution of the geomagnetic field. Among them the hemispheric asymmetry of the magnetic field [38] which is responsible for a more intense radial field at the longitude of about 150° E [29], the same as the current longitude of the eccentric dipole [65] and close to that of the hypothesized IC displacement. Movements of the IC in the equatorial plane could also be related to the gravity variations induced by core flows [25] and the correlations between magnetic and gravity anomalies at low and middle latitudes recently reported by Mandea et al. [56].

In the following we discuss in more detail four such geophysical phenomena and we show that the hypothesis of a decentered IC could contribute to their explanation.

A. The anomalous layer at the bottom of the OC

At the bottom of the OC seismological data reveal an anomaly consisting of PKPbc-PKIKP residuals smaller than predicted by reference one-dimensional models [95]. This anomaly has been interpreted as a layer of low velocity gradient in the lowermost 150-200 km of the OC [81, 95], which could delay the PKIKP travel time and produce smaller PKPbc-PKIKP residuals [95]. The favored explanation of this anomaly is the existence of a stably stratified region resulting from a dynamic equilibrium between the production of iron reach melt and mixing with light fluid [21, 81]. Melting may occur through the formation of a positive topography at the ICB by translational IC convection [1, 58], provided that the OC convection supplies the necessary latent heat, or by OC convection itself, when the temperature in the surrounding OC fluid is locally larger than at the ICB [34]. However, both mechanisms suffer of limitations and there is no definitive proof that they are self-sustaining [21].

The hypothesis of an eccentric IC could contribute to more appropriate explanation of this anomalous layer from a new perspective. The IC displacement over approximately 100 km should produce noticeable effects at the bottom of the OC. If r_c is the radius of the IC, then the distances from the Earth's center to the ICB vary between $r_c - 100$ and $r_c + 100$. Hence the observed anomalous layer contains this spherical shell with an inhomogeneous material structure which should be taken into account to explain the seismical data. For example, the observed PKPbc-PKIKP and PKiKP-PKIKP differential travel time anomalies, which can be simultaneously explained by different radial velocity gradients at the bottom of the OC in the two hemispheres [95, 96], could be related to the different lengths of the PKIKP path inside a decentered IC.

There may be other seismic observations related to this region of the OC. For instance, if the IC is decentered, while the seismic model assumes that it is centered, then the interpretation of the seismic observations would have larger errors in the spherical layer of 200 km containing the ICB than in other regions of the OC. Indeed, the reference one-dimensional seismic models are different from each other over a thickness of roughly 200 km above ICB [81, 95, 96].

B. Differential rotation of the IC and the hemispheric seismic asymmetry

The flow in the fluid OC and the angular momentum conservation induce changes in the angular velocity and rotation axis of the IC [3, 27, 83]. The differential rotation of the IC, first predicted from theoretical considerations [33], was obtained by geodynamo numerical simulations in the mid-nineties [31]. But the differential rotation of the IC is hardly compatible with the current explanations of the hemispheric dichotomy (see Sects. III and IV). If the ATIC and the observed hemispheric attenuation anomaly are explained by solidification texturing controlled by the mantle [3], a differential rotation faster than a full revolution in a few hundreds of millions of years would erase any longitudinal signature in the texturing [21, 26].

In order to avoid this contradiction, the recent dynamo models adjust the viscous, magnetic, or gravitational torques such that the present day mean rotation rate appears as a temporal fluctuation superposed over a very slow steady super rotation of a few degrees per million years [5, 26] or even without offset of steady super

rotation over long timescales [27]. However, this is yet not a satisfactory solution, since the longitudinal variations of the solidification rates interacting with mantle heterogeneities can result in a gravitationally driven differential rotation of the IC in the westward direction [26], opposite to that of the rotation suggested by seismic observations, which could be too fast to preserve longitudinal differences in texturing [21].

Another tentative explanation for ATIC and the attenuation anomaly is a convective west-east translation of the IC [1, 58], with minimal influence of the mantle on the core dynamics [21, 88] (see Appendix A). This theory considers that the IC is shifted by 100 m from the Earth's center. But then, the viscous momentum due to the OC flow near the asymmetric ICB should modify the rate and the axis of the differential rotation, hindering the onset of the internally driven convective translation. An additional difficulty of this approach is the fact that flows derived from geomagnetic observations and dynamo simulations reproducing patterns of geomagnetic secular variation predict opposite IC translations from east to west [4, 6].

The decentered IC hypothesis avoids these contradictions because both the ATIC and the hemispheric asymmetry of the attenuation are explained by the displacement of the IC, without any constrains on its internal structure (Sects. III and IV). Then the IC can rotate with respect to the mantle with any angular velocity around any axis. Therefore our hypothesis does not rule out any of the different existing estimations of the angular velocity of the differential rotation which are listed below.

Early geodynamo predictions of a super-rotation of the IC by $2-3^\circ$ per year induced by magnetic and viscous torques exerted by the eastward zonal flow near the IC [31] were found in reasonable agreement with seismic data. Travel time anomalies of the PKIKP phase indicated a differential rotation rate of $\sim 3^\circ$/yr [83] while travel time residuals of the PKIKP rays with respect to seismic rays turning at the base of the OC (PKPbc) indicated a rate of $\sim 1^\circ$/yr [79]. Subsequent studies, using earthquake doublets, normal modes, and refined methods favor much smaller rotation rates between 0.0°/yr and 0.3°/yr or even a retrograde, westward, rotation [81]. Observations of temporal trends of PKPbc-PKIKP residuals, similar to previous studies [79] but using earthquakes produced in four different source regions, were found to be consistent with both eastward and westward differential IC rotation in different regions, suggesting that differential IC rotations of tenths of degrees per year are incompatible with global data [57]. On the other hand, an inverse analysis of doublets observed at College station over more than forty years [88] found an average differential rotation of $0.25-0.48^\circ$/yr and decadal fluctuations of the order of 1°/yr. These results are consistent with the observed decadal changes in the length of the day [88], which in turn indicate the presence of zonal flows in the fluid core, as required by the currently accepted mechanism of the IC differential rotation [21, 31], as well as with decadal changes in the magnetic field which may be responsible for the observed fluctuations in the IC rotation [54].

C. Large-scale anomalies of the geoid

A displacement of the IC over tens of kilometers should produce a measurable effect on the gravitational field at the Earth's surface. A simple calculation shows that for an IC displacement of 1 km, the surface of the geoid (the gravity equipotential that coincides with sea level) changes by 1 m. The largest negative geoid anomaly has -103 m and lies south of India while the largest positive one has 80 m and occurs near New Guinea. Hence the magnitude of the observed anomalies corresponds to a displacement of about 100 km, but their distribution has no explicit correlation with the theoretical gravitational field of a displaced IC. At first sight, the observed anomalies lack the necessary rotational symmetry around the displacement direction of the IC determined in the previous sections.

However, Barta [7] showed that the geoid anomalies can be well approximated at large-scale by a superposition of two global anomalies with cylindrical symmetries around axis directed toward the centers of the two greatest geoid anomalies

$$\Sigma_1(\theta,\phi) = -\ \ 0.3 - \ 3.70\,P_2(\theta_1) - 46.11\,P_3(\theta_1) + \ \ 8.16\,P_4(\theta_1) + 15.56\,P_5(\theta_1)$$
$$\Sigma_2(\theta,\phi) = -11.8 + 61.74\,P_2(\theta_2) + 43.50\,P_3(\theta_2) - 25.13\,P_4(\theta_2) - \ \ 5.10\,P_5(\theta_2),$$

where P_i are the Legendre polynomials of order i. The angles θ_1 and θ_2 are the angles between the radius with the geographical coordinates (θ,ϕ) and the axis pointing to the directions of 58 °E and 156.5 °E in the equatorial plane, respectively. In this way, instead of several anomalies, we have to explain only two global anomalies which already have the necessary cylindrical symmetry. Barta ascribed Σ_2 to an eastward shift of the IC over 100 km [9]. But the gravitational anomaly generated by the shifted IC alone is dominated by the term containing $P_1(\theta_1) = cos\theta_1$ which is absent in the formula for Σ_2.

The explanation of the geoid anomalies Σ_1 and Σ_2 could be obtained by the mechanism of the dynamic topography. This is the usual method to derive the longest

wavelength components of the residual geoid [36]. The seismically-inferred density contrasts in the lower mantle are negatively correlated with the observed geoid. Therefore one needs a counteracting effect, called dynamic topography: the thermally driven convective flow in the mantle induces deformations of Earth's surface and of the CMB which count as negative masses [68]. The strength of such a mechanism generating large-scale density variations inside the OC is however disputed [11].

Theoretical estimations indicate that dynamical forces originating inside the OC cannot support any appreciable internal structure [82]. But this is not true if there exists a non-hydrostatic forcing due to gravitational interactions with the exterior mass distributions or to boundary effects [91]. As we pointed out in Sect. II B, such a non-hydrostatic forcing could be generated by the decentered IC. The results of seismological investigations are contradictory. Some studies exclude any large-scale aspherical structure inside the OC [10, 43, 52, 80], while others have found significant cylindrical structures related to the tangent cylinder (see Sect. II A) [72, 73] or non-homogeneous structures inside the OC [19, 70, 78].

Hence, the eastward displacement of the IC could cause a temperature increase in the Eastern Hemisphere and implicitly a density decrease. In addition, it could induce large-scale inhomogeneities in the mantle structure and variations of the CMB depth. These hemispheric asymmetries could compensate the IC displacement explaining the absence of the term $P_1(\theta_1)$ in Σ_2. This interpretation is in accordance with Bowin's estimation that the second order term, which dominates the expression of Σ_2, has the origin at depths of 6000 km, i.e., inside the IC [11, Fig. 8]). The third degree term, dominating the expression of Σ_1, originates at 3000 km depth, in the neighborhood of CMB. In this way the large-scale anomalies of the geoid are explained by two global density anomalies, one determined by an eccentric IC, the other related to the topography of the CMB and corresponding to the boundary conditions used in the numerical simulation of the geodynamo [6], discussed in Sect II A.

D. Hemispherical asymmetry of the IC anisotropy

The elastic anisotropy of the IC is characterized by P-waves travel times about 3% faster in the polar direction than parallel to the equatorial plane. According to many seismic studies, the first 150 km beneath the ICB have low levels of anisotropy (smaller than 1%) and the uppermost 50-90 km form an isotropic layer [41, 81] (see Sect. III). Anisotropy has been clearly documented only at depths of several hundreds of kilometers [41, 60, 81]. While the anisotropy in the innermost IC presented no significant longitudinal dependence [42, 60], hemispherical patterns were observed at depths above 600-700 km, with an anisotropic Western Hemisphere and a nearly isotropic eastern one [24], with anisotropy levels of 4.4% and 1%, respectively [41]. Recently, based on an extensive data set of PKIKP travel times, Lythgoe et al. conclude that there is no clear evidence of an innermost IC and the hemispherical variation of the anisotropy extends through the entire IC [55].

There exist several theories regarding the generation of the IC anisotropy with hemispherical variations [86]. If it results from hemispheric variations in the IC growth, then a mechanism is needed to produce different solidification rates and crystalline structures inside the IC. This mechanism could be controlled by interactions of the IC with the rest of the Earth, for instance, by the OC flow caused by thermal inhomogeneities in the mantle [86]. To ensure a constant influence on the IC growth through such mechanisms, the IC should be locked to the mantle for at least 200 million years [41], at variance with the currently accepted theories on differential rotation (see Sect. VI B).

The hemispherical asymmetry in anisotropy of the IC is the mostly used explanation for the complexity of the seismological observations, but not the only one available. For example, Romanowicz and Bréger showed that anomalous splitting of most of the normal modes sensitive to the interior structure of the IC, excepting a single one, can be explained either by considering an asymmetric IC anisotropy or an inhomogeneous OC structure [72]. Indeed, polar regions of the OC with seismic velocities larger than the velocities near the equatorial plane generate an anisotropy of PKIKP travel times similar to that generated by an anisotropic structure of the IC. Such an inhomogeneous OC is consistent with the simulated flow inside the OC (Sect. II A), which has different characteristics outside the tangent cylinder and near the rotation axis, as well as with the density inhomogeneities in the OC discussed in Sect. VI C. Hence a decentred IC could be a part of a complete explanation of the hemispherical asymmetry of the IC anisotropy.

VII. CONCLUSIONS

An IC displaced by tens of kilometers from the Earth's center should influence many mechanical, thermal, and magnetic phenomena in the Earth's interior. In this paper we have analyzed several of them:

- secular westward drift of the geomagnetic field at low latitudes (Sect. II A);
- global asymmetries of the flow and magnetic field inside the OC (Sect. II A);
- nonhydrostatic shape of the Earth (Sect. II B);
- Markowitz wobble of the Earth's pole (Sect. II B);
- decadal variations of the length of day (Sect. II B);
- translational oscillations of the IC (Slichter mode) (Sect. II C);

- isotropic hemispheric asymmetry of the travel times at the top of the IC (Sect. III);
- hemispheric asymmetry of the attenuation at the top of the IC (Sect. IV);
- hemispheric asymmetry of the precritical PKiKP travel times (Sect. V);
- anomalous layer at the bottom of the OC (Sect. VI A);
- differential rotation of the IC (Sect. VI B);
- large-scale anomalies of the geoid (Sect. VI C);
- density heterogeneities inside the OC (Sect. VI C);
- anisotropy of the IC (Sect. VI D).

We have approached most of the above issues qualitatively and explained two of them (ATIC and the attenuation asymmetry) through rigorous numerical simulations of differential travel times sampling the top of the IC. In conclusion, we estimate that the displacement of the IC could be larger than 3 km and smaller than 100 km, most likely equal to several tens of kilometers. The estimated direction of the displacement varies between 110 °E and 160 °E. The time scale of the translational motion of the IC could be larger than several hundreds of years. The resulting picture is that of a perturbation generated by the decentered IC which enhances the nonequilibrium and the nonhydrostaticity of the well-established basic structure of the Earth. We consider that more flexible dynamical models of the Earth's interior could be obtained by simply letting the IC to participate in the movement of the OC.

It is tempting to adopt such a simple solution for a wide variety of disputed geophysical problems. But for each individual phenomenon there are many other perturbations making it difficult to obtain a clear separation of the effects of a decentered IC. Nevertheless, we believe that the numerous implications discussed in this article are convincing enough and that this hypothesis deserves further exploration.

Appendix A: History of the eccentric IC hypothesis

The hypothesis of an eccentric IC with respect to the mass center of the Earth has been launched for the first time in 1970s. At that time the seismical observations were not providing enough information on the Earth's structure near the ICB. Therefore indirect observations regarding the gravity and geomagnetic fields or the distribution of the crust inhomogeneities were used.

Barta interpreted the displacement of the dipole of the geomagnetic field toward Australia as an indication for an eccentric IC [7–9]. Assuming that the density of the OC is larger in the displacement direction, he found that the distance between the IC and the Earth's rotation axis is of the order of 100 km. He discussed the implications of such a configuration on the magnetic secular variation, on the connection between the magnetic and gravity fields, and on the deviation of the geoid figure from the hydrostatic equilibrium.

From paleomagnetic data, Zidarov reached the conclusion that "the optimal magnetic dipole was located away from the Earth's center during the geological past" and, in consequence, "the core itself was located in the geological past away from the Earth's center, toward the middle of the Pacific Ocean and gradually shifted toward its center" [97]. Using the difference between the equatorial moments of inertia of the Earth, he computed a displacement of the IC of 35 km. He also discussed several other effects of an eccentric IC on the piriform shape of the Earth, the opening rate of the oceans, the geographic pole wandering, the contemporary geotectonic activity, and the continental drift.

Vesanen and Teisseyre analyzed the deviations from symmetry of the earthquake zones and interpreted them as an indication for the existence of some deep asymmetry inside the Earth [90]. They also applied Barta and Zidarov's approaches to assess the influence of an eccentric IC on the pattern of convection cells in the Earth's interior.

A recently proposed mechanism which explains the hemispheric ATIC (see Sect. III) assumes an eastward translation of the IC as a result of crystallization in the Western Hemisphere and melting in the Eastern Hemisphere in a superadiabatic regime [1, 2, 58, 59]. In this process, the IC center of mass is shifted toward its colder and denser Western Hemisphere [58]. In an attempt to restore the mechanical equilibrium, the IC as a whole will then be shifted toward east. The eastward shift of the IC was estimated at about 100 m in the equatorial plane [1]. This shift produces a positive topography on the Eastern Hemisphere of the ICB which melts by exchange of latent heat with the OC fluid and, at the same time, forces crystallization on the western IC hemisphere. A continuous translation mechanism could result from the interaction of superadiabaticity, gravitational equilibrium, and latent heat exchange with the OC [2]. The increase of the iron grain-size during the west-east convective translation of the IC could explain the observed hemispheric asymmetry of travel times and attenuation.

Currently accepted parameters of the Earth's interior (e.g. viscosity, IC age) impose constraints on the onset of this mechanism [21] and it is currently difficult to reach firm conclusions on the possibility of convection in the actual IC [22]. Nevertheless, it is possible that conditions for convection were met at early stages generating the seismical asymmetry and anisotropy observed in the deeper parts of the IC [12, 17]. In addition, the results of recent geodynamo modeling of the geomagnetic secular variation are rather consistent with a translation of the IC in the opposite, east-west direction [4, 6]. Another difficulty encountered by the proposed continuous convection mechanism is the assumption that the IC is in

mechanical equilibrium with the surrounding fluid OC. The interaction of the flow at the bottom of the OC with the positive topography of the ICB would induce a supplementary rotation of the IC, at variance with the static equilibrium and the fixed direction of the convective translation predicted by the theory.

Appendix B: Numerical model

Since we focus only on the effect of a decentered inner core on the propagation of the seismic rays, we consider a numerical model as simple as possible so that other perturbing effects are disregarded. Therefore, we keep most of the spherical symmetry of the Earth's structure, even in case of a displaced inner core. The surfaces of the Earth and of the inner core are spheres and the velocity profile inside them is that of the one-dimensional model ak135 [49]. Outside the decentered inner core, the model ak135 is linearly extrapolated to the points of the outer core situated at distances from the Earth's center smaller than the inner core radius. In this way we alter as little as possible the model with spherical symmetry of the Earth's interior, maintaining the symmetry separately for the inner core and the rest of the Earth.

The inner core interior and the rest of the Earth are divided into spherical layers with constant velocity of maximum 1 km thickness. The reference levels of the ak135 model are all included among the boundaries of spherical layers. Therefore the numerical seismic rays are made of straight segments satisfying the refraction and reflection laws at the boundaries of the spherical layers. The propagation plane of the seismic ray changes only at the incidence with the inner core boundary, which separates the two volumes with spherical symmetry into the interior and exterior of the inner core. The numerical errors of the travel time for a centered inner core obtained with this numerical algorithm with respect to the values given in seismological tables [48] are of the order of 0.01 s, i.e., one order of magnitude smaller than the residuals characterizing the ATIC (Sect. III).

In order to construct the seismic ray we have to specify the position of the earthquake focus and the initial propagation direction of the ray. We first fix the latitude $\phi_{\rm C}$ and the longitude $\lambda_{\rm C}$ of the point C defined by the intersection with the Earth's surface of the straight line through the center O of the Earth and the center $\rm O_C$ of the displaced inner core intersects the Earth's surface (Fig. 7). To avoid an intricate three-dimensional graphical representation we use a double projection: first a central projection on the Earth's surface from its center O and then an orthogonal projection on the meridian plane containing the axis OC defined by the displacement of the inner core.

The epicenter E is the projection of the earthquake focus on the Earth's surface and $\rm E_C$ in Fig. 7 is the projection of E on the meridian plane. The position of the epicenter E in the plane OEC is given by the angle $\delta_{\rm E}$

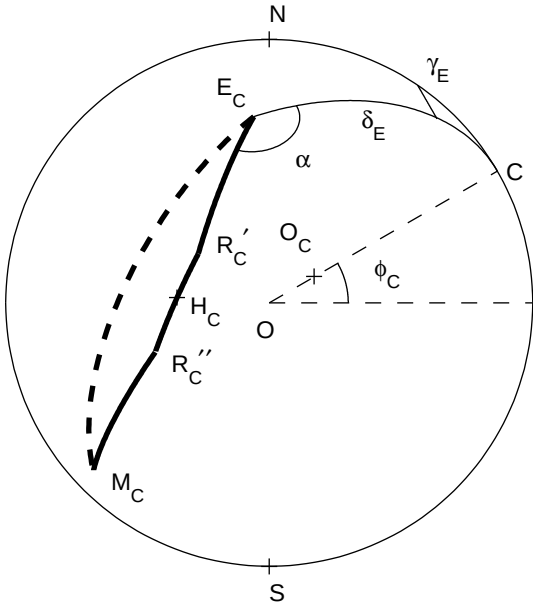

FIG. 7. Double projection (on the Earth's surface and on the meridian plane containing the center of the decentered inner core) of the $\rm PKiKP_{dec}$ seismic ray. The dashed line is the double projection of the PKIKP ray with the same focus and exit points in case of the centered inner core. The meaning of the points and angles notations are given in text.

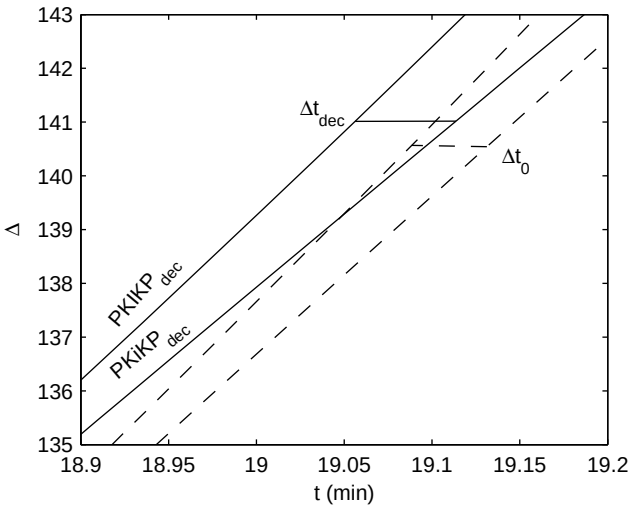

FIG. 8. Seismic diagram for a displaced inner core. Epicentral distance versus travel time for the $\rm PKIKP_{dec}$ and $\rm PKiKP_{dec}$ rays in the Eastern Hemisphere plotted in Fig. 1 (continuous lines) and for the PKIKP and PKiKP rays corresponding to a centered inner core (dashed lines).

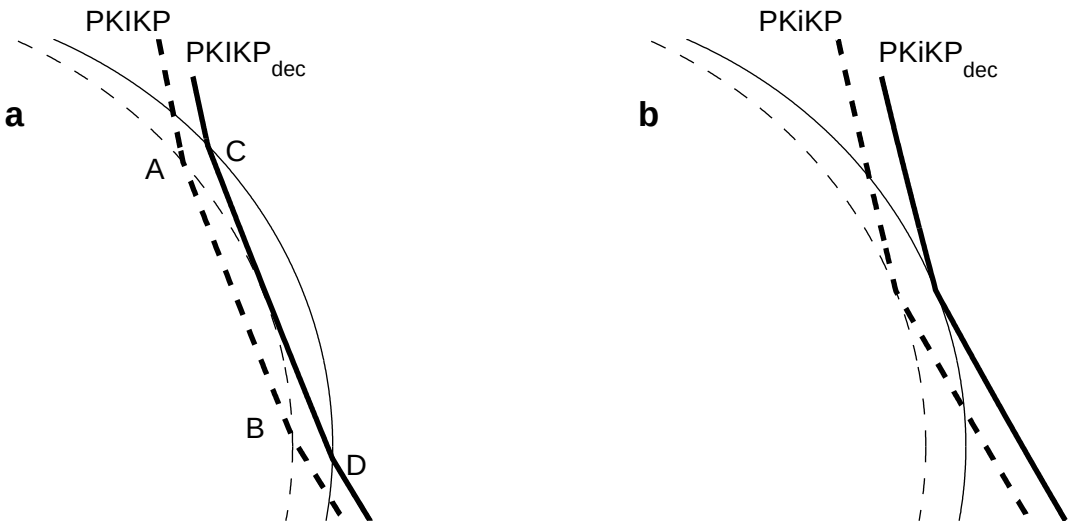

FIG. 9. Seismic rays in the neighborhood of the inner core boundary. The seismic rays have the same focus and exit point and propagate in the meridian plane containing the center of the inner core displaced in the Eastern Hemisphere as in Fig. 1. The refracted rays (a) and the reflected ones (b) are plotted with thick continuous lines for the decentered inner core and with thick dashed lines for the centered inner core. The circular arcs represent boundaries of the decentered (continuous line) and centered (dashed line) inner core.

between the radii OE and OC. The angle between the OEC plane and the meridian plane NCS is denoted by $\gamma_{\rm E}$. The propagation of the seismic ray has a cylindrical symmetry with respect to the OC axis, its shape being independent of the angle $\gamma_{\rm E}$.

Because of the spherical symmetry of the Earth's interior above the inner core boundary, the seismic ray keeps its propagation plane until it reaches the inner core boundary at the point $\rm R^{'}$. The propagation plane changes under reflection and refraction at the inner core boundary. The $\rm PKIKP_{dec}$ phase propagates through the displaced inner core with spherically symmetric internal structure in the plane $\rm OR^{'}R^{''}$ where $\rm R^{''}$ is the exit point on the inner core boundary. After the second refraction on the inner core boundary, outside the inner core it propagates in the plane $\rm OMR^{''}$, where M is the exit point on the Earth's surface. The $\rm PKiKP_{dec}$ seismic ray changes its propagation plane once, at reflection on the inner core boundary at the point $\rm R^{'}$.

In Fig. 7 the double projection $\rm E_C R^{'}_C R^{''}_C M_C$ of $\rm PKIKP_{dec}$ seismic ray is composed by three parts separated by the deflection points where the seismic ray is refracted by the inner core boundary. The initial propagation plane $\rm OER^{'}$ of the seismic ray is specified by the angle α with the plane OEC. The initial direction of propagation in this plane is given by the incidence angle between the ray and the normal to the Earth's surface in E (not shown in the figure).

A special situation occurs when the seismic ray propagates in the OEC plane ($\alpha = 0$ or $\alpha = \pi$). Then, the normal to the inner core boundary at $\rm R^{'}$ belongs to the propagation plane, which does not change by reflection or refraction at the inner core boundary. The seismic rays for the same initial incident angle clearly exhibit an east-west asymmetry, as shown in Fig. 1 for an eastward displacement of the inner core in the equatorial plane ($\lambda_{\rm C} = \pi/2$ and $\phi_{\rm C} = 0$) and for epicenter at the North Pole ($\delta_{\rm E} = \pi/2$).

When the inner core is decentered, the epicentral distance and the travel time of the $\rm PKIKP_{dec}$ and $\rm PKiKP_{dec}$ phases depend on the initial propagation plane of the seismic ray and on the location of the earthquake focus. First we analyze the simple situation presented in Fig. 1 when the seismic ray is contained in the plane OCE and the inner core is shifted by 100 km toward 90° E ($\lambda_{\rm C} = \pi/2$ and $\phi_{\rm C} = 0$). For a focus depth of 200 km, we have generated seismic rays with epicentral distance in the same interval as that investigated in [92, 93]. The corresponding seismic diagram is presented in Fig. 8. We have chosen the PKIKP rays propagating in the region toward which the inner core is shifted ($\alpha = 0$), so that their path into the inner core is longer than for a centered inner core. The diagrams for both $\rm PKIKP_{dec}$ and $\rm PKiKP_{dec}$ phases are shifted toward smaller travel times with a different amount, so that the distance between diagrams changes and the residuals $\Delta t_{\rm dec} - \Delta t_0$ are non-vanishing.

To explain the changes in seismic diagrams caused by the displacement of the inner core, we plot in Fig. 9 the paths in the neighborhood of the inner core boundary of the seismic rays which emerge at the same point on the Earth's surface at $\Delta = 140°$. Because of the shifted position of the inner core, the total lengths, from the focus to the common exit point, of the $\mathrm{PKIKP_{dec}}$ and $\mathrm{PKiKP_{dec}}$ rays are smaller than those for a centered inner core (dashed lines) with approximately the same amount. These shorter paths explain the smaller travel times of the seismic phases for a decentered inner core, but not the non-vanishing residuals $\Delta t_{\mathrm{dec}} - \Delta t_0$.

There is another geometric effect which modifies the differential travel time Δt_{dec}. The segment CD of the seismic ray within the decentered inner core is longer than the segment AB for the centered inner core (Fig. 9a). Because the velocity in the inner core is larger than in the outer core, the travel time of the $\mathrm{PKIKP_{dec}}$ phase has an additional decrease, the differential travel time Δt_{dec} increases, and the residual $\Delta t_{\mathrm{dec}} - \Delta t_0$ becomes positive. In the diametrically opposite region of the inner core the distance CD is smaller than AB and the residual is negative, resulting in a hemispheric asymmetry. Hence, the asymmetry of the residuals of the differential travel time can be explained by the variation of the $\mathrm{PKIKP_{dec}}$ ray paths in the decentered inner core without modifying the seismic velocities.

In order to obtain the geographical distribution of the ATIC residuals plotted in Fig. 3 we compute them for earthquakes evenly distributed on the Earth's surface and seismic rays uniformly distributed around the focus. More precisely, we specify the position of the inner core by fixing the angles λ_{C} and ϕ_{C} and the distance between the center of the inner core and the center of the Earth to $d = 100$ km. The angles γ_{E}, δ_{E}, and α are then varied by steps of 10°. For given values of δ_{E} and α, we construct the seismic ray with turning point at the depth of 39 km and we calculate the corresponding residual. Because of the cylindrical symmetry the shape of the seismic ray does not depend on γ_{E}. For each seismic ray we determine the geographical coordinates of the turning point H ($\mathrm{H_C}$ in Fig. 7 is its double projection).

[1] T. Alboussiere, R. Deguen, M. Melzani, *Melting-induced stratification above the Earth's inner core due to convective translation*, Nature 466, 744-747 (2010).

[2] T. Alboussiere, R. Deguen, *Asymmetric dynamics of the inner core and impact on the outer core*, J. Geodyn. 61, 172-182 (2012).

[3] J. Aubert, H. Amit, G. Hulot, P. Olson, *Thermochemical flows couple the Earth's inner core growth to mantle heterogeneity*, Nature 454, 758-761 (2008).

[4] J. Aubert, *Flow throughout the Earths core inverted from geomagnetic observations and numerical dynamo models*, Geophys. J. Int. 192, 537-556 (2013).

[5] J. Aubert, D. Dumberry, *Steady and fluctuating inner core rotation in numerical geodynamo models*, Geophys. J. Int. 184, 162-170 (2011).

[6] J. Aubert, C.C. Finlay, A. Fournier, *Bottom-up control of geomagnetic secular variation by the Earths inner core*, Nature 502, 219-223 (2013).

[7] G. Barta, *Physical background of the geoidal figure*, Nature 243, 156 (1973).

[8] G. Barta, *Satellite geodesy and the internal structure of the earth*, in *Space research XIV*, Eds. M.J. Rycroft and R.D. Reasenberg, Akademie-Verlag, Berlin (1974).

[9] G. Barta, *Recent results of the study of physical background of the geoidal figure*, Adv. Space Res. 1, 195 (1981).

[10] L. Boschi, A.M. Dziewonski, *Whole earth tomography from delay times of P, PcP, and PKP phases: Lateral heterogeneities in the outer core or radial anisotropy in the mantle?*, J. Geophys. Res. 105, 13675-13696 (2000).

[11] C. Bowin, *Mass anomaly structure of the earth*, Review of Geophysics 38, 355-387 (2000).

[12] B.A. Buffett, *Onset and orientation of convection in the inner core*, Geophys. J. Int. 179, 711-719 (2009).

[13] B. A. Buffett, J. Bloxham, *Deformation of Earth's inner core by electromagnetic forces*, Geophys. Res. Lett. 27, 4001-4004 (2000).

[14] B. A. Buffett, G. A. Glatzmaier, *Gravitational braking of inner core rotation in geodynamo simulations*, Geophys. Res. Lett. 27, 3125-3128 (2000).

[15] A. Cao, B. Romanowicz, *Hemispherical transition of seismic attenuation at the top of the Earth's inner core*, Earth Planet. Sci. Lett. 228, 243-253 (2004).

[16] U.R. Christensen, J. Wiht, *Numerical Dynamo Simulations*, in *Treatise on Geophysics*, Vol. 8, *Core Dynamics*, edited by G. Schubert, P. Olson, 245-282, Elsevier, Amsterdam (2007).

[17] V. F. Cormier, *Texture of the uppermost inner core from forward- and back-scattered seismic waves*, Earth Planet. Sci. Lett. 258, 442-453 (2007).

[18] V. F. Cormier, J. Attanayake, K. He, *Inner core freezing and melting: Constraints from seismic body waves*, Phys. Earth Planet. Int. 188, 163-172 (2011).

[19] W. Dai, X. Song, *Detection of motion and heterogeneity in Earth's liquid outer core*, Geophys. Res. Lett. 35, L16311 (2008).

[20] Z. Dai, W. Wanga, L. Wen, *Irregular topography at the Earths inner core boundary*, PNAS 109, 7654-7658 (2012).

[21] R. Deguen, *Structure and dynamics of Earths inner core*, Earth Planet Sci. Lett. 333-334, 211-225 (2012).

[22] R. Deguen, P. Cardin, *Thermochemical convection in Earths inner core*, Geophys. J. Int. 187, 1101-1118 (2011).

[23] V. Dehant, P.M. Mathews, *Earth rotation variations*, in *Treatise on Geophysics*, Vol. 3, *Geodesy*, edited by G. Schubert, T.A. Herring, 239-294, Elsevier, Amsterdam (2007).

[24] A. Deuss, J.C.E. Irving, J. H. Woodhouse, *Regional variation of inner core anisotropy from seismic normal mode observations*, Science 328, 1018-1020 (2010).

[25] M. Dumberry, *Gravity variations induced by core flows*, Geophys. J. Int. 180, 635–650 (2010).

[26] M. Dumberry, *Gravitationally driven inner core differen-*

tial rotation, Earth Planet. Sci. Lett. 297, 387-394 (2010).

[27] D. Dumberry, J. Mound, *Inner core-mantle gravitational locking and the super-rotation of the inner core*, Geophys. J. Int. 181, 806-817 (2010).

[28] E.R. Engdahl, R. van der Hilst, R. Buland, *Global teleseismic earthquake relocation with improved travel times and procedures for depth determination*, Bull. Seismol. Soc. Am. 88, 722-743 (1998).

[29] Y. Gallet, G. Hulot, A. Chulliat, A. Genevey, *Geomagnetic field hemispheric asymmetry and archeomagnetic jerks*, Earth Planet. Sci. Lett. 284, 179-186 (2009).

[30] R. Garcia, A. Souriau, *Inner core anisotropy and heterogeneity level*, Geophys. Res. Lett. 27, 3121-3124 (2000).

[31] G.A. Glatzmaier, P. H. Roberts, *Rotation and magnetism of Earth's inner core*, Science 274, 1887-1891 (1996).

[32] R.S. Gross, *Earth rotation variations - long period*, in *Treatise on Geophysics*, Vol. 3, *Geodesy*, edited by G. Schubert, T.A. Herring, 239-294, Elsevier, Amsterdam (2007).

[33] D. Gubbins, *Rotation of the inner core*, J. Geophys. Res. 86, 11695-11699 (1981).

[34] D. Gubbins, B. Sreenivasan, J. Mound, S. Rost, *Melting of the Earths inner core*, Nature 473, 361-363 (2011).

[35] C.R. Gwinn, T.A. Herring, I.I. Shapiro, *Geodesy by radio interferometry: Studies of the forced nutations of the Earth, 2. Interpretation*, J. Geophys. Res. 91, 4755-4765 (1986).

[36] B.H. Hager, R.W. Clayton, M.A. Richards, R.P. Comer, A.M. Dziewonski, *Lower mantle heterogeneity, dynamic topography and the geoid*, Nature 313, 541 (1985).

[37] R. Holme, *Large-scale flow in the core*, in *Treatise on Geophysics*, Vol. 8, *Core Dynamics*, edited by G. Schubert, P. Olson, 107-130, Elsevier, Amsterdam (2007).

[38] G. Hulot, c. Eymin, B. Langlais, M. Mandea, N. Olsen, *Small scale structure of the geodynamo inferred from Oersted and Magsat satellite data*, Nature 416, 620-623, (2002).

[39] International Seismological Centre, On-line Bulletin, http://www.isc.ac.uk, Internatl. Seis. Cent., Thatcham, United Kingdom (2013).

[40] R. Iritani, N. Takeuchi, H. Kawakatsu, *Seismic attenuation structure of the top half of the inner core beneath the northeastern Pacific*, Geophys. Res. Lett. 37, L19303 (2010).

[41] J.C.E. Irving, A. Deuss, *A Hemispherical structure in inner core velocity anisotropy*, J. Geophys. Res. 116, B04307 (2011).

[42] M. Ishii, A. M. Dziewoński, *The innermost inner core of the earth: Evidence for a change in anisotropic behavior at the radius of about 300 km*, PNAS 99, 14026-14030 (2002).

[43] M. Ishii, A.M. Dziewonski, *Constraints on the outer-core tangent cylinder using normal-mode splitting measurements*, Geophys. J. Int. 162, 787-792 (2005).

[44] A. Jackson, *Intense equatorial flux splots on the surface of the earths core*, Nature 424, 760763 (2003).

[45] A. Jackson, C.C. Finlay, *Geomagnetic secular variation and its application to the core*, in *Treatise on Geophysics*, Vol. 5, *Geomagnetism*, edited by G. Schubert, M. Kono, 147-193, Elsevier, Amsterdam (2007).

[46] G. Jiang, D. Dapeng Zhao, *Observation of high-frequency PKiKP in Japan: Insight into fine structure of inner core boundary*, J. Asian Earth Sci. 59, 167-184 (2012).

[47] H. Kawakatsu, *Sharp and seismically transparent inner core boundary region revealed by an entire network observation of near-vertical PKiKP*, Earth Planets Space 58, 855-863 (2006).

[48] B.L.N. Kennett, *Seismological Tables: ak135*, The Australian National University Canberra ACT 0200 Australia (2005).

[49] B. Kennett, E. Engdahl, and R. Buland, *Constraints on seismic velocities in the Earth from travel times*, Geophys. J. Int. 122, 108-124 (1995).

[50] K.D. Koper, M.L. Pyle, J.M. Franks, *Constraints on aspherical core structure from PKiKP-PcP differential travel times*, J. Geophys. Res. 108, 2168 (2003).

[51] I. Lehman, *P'*, Publications du Bureau Central Séismologique International A 14, 87-115 (1936).

[52] D. Leykam, H. Tkalčić, and A.M. Reading, *Core structure re-examined using new teleseismic data recorded in Antarctica: evidence for, at most, weak cylindrical seismic anisotropy in the inner core*, Geophys. J. Int. 180, 1329-1343 (2010).

[53] X. Li, V.F. Cormier, *Frequency-dependent seismic attenuation in the inner core 1. A viscoelastic interpretation*, J. Geophys. Res. 107, 2361 (2002).

[54] P. W. Livermore, R. Hollerbach, A. Jackson, *Electromagnetically driven westward drift and inner-core superrotation in Earths core*, PNAS 110.40, 15914-15918 (2013).

[55] K.H.Lythgoe, A. Deuss, J.F. Rudgea, J.A. Neufeld, *Earths inner core: Innermost inner core or hemispherical variations?*, Earth Planet. Sci. Lett. 385, 181-189 (2014).

[56] M. Mandea, I. Panet, V. Lesur, O. de Viron, M. Diament, J-L. Le Mouël, *Recent changes of the Earth's core derived from satellite observations of magnetic and gravity fields*, PNAS 109.47, 19129-19133 (2012).

[57] A. M. Mäkinen, A. Deuss, *Global seismic body-wave observations of temporal variations in the Earths inner core, and implications for its differential rotation*, Geophys. J. Int. 187, 355-370 (2011).

[58] M. Monnereau, M. Calvet, L. Margerin, A. Souriau, *Lopsided growth of Earth's inner core*, Science 328, 1014-1017 (2010).

[59] H. Mizzon, M. Monnereau, *Implication of the lopsided growth for the viscosity of Earths inner core*, Earth Planet. Sci. Lett. 361, 391-401 (2013).

[60] F. Niu, Q. Chen, *Seismic evidence for distinct anisotropy in the innermost inner core*, Nature Geoscience 1, 692-696 (2008).

[61] F. Niu, L. Wen, *Hemispherical variations in seismic velocity at the top of the Earth's inner core*, Nature 410, 1081-1084 (2001).

[62] T. Ohtaki, S. Kaneshima, K. Kanjo, *Seismic structure near the inner core boundary in the south polar region*, J. Geophys. Res. 117, B03312 (2012).

[63] E.A. Okal, S. Stein, *Observations of ultra-long period normal modes from the 2004 SumatraAndaman earthquake*, Phys. Earth Planet. In. 175, 5362 (2009).

[64] N. Olsen, G. Hulot, T.J. Sabaka, *The Present Field*, in *Treatise on Geophysics*, Vol. 5, *Geomagnetism*, edited by G. Schubert, M. Kono, 147-193, Elsevier, Amsterdam (2007).

[65] P. Olson, R. Deguen, *Eccentricity of the geomagnetic dipole caused by lopsided inner core growth*, Nature Geoscience 5, 565-569 (2012).

[66] S.I. Oreshin, L.P. Vinnik, *Heterogeneity and anisotropy of seismic attenuation in the inner core*, Geophys. Res. Lett. 31, L02613 (2004).

[67] A. Ouzounis, K. Creager, *Isotropy overlying anisotropy at the top of the inner core*, Geophys. Res. Lett. 28, 4331-4334 (2001).

[68] C.L. Pekeris, *Thermal convection in the interior of the Earth*, Mon. Not. R. Astron. Soc., suppl. 3, 343-367 (1935).

[69] Z. Peng, K.D. Koper, J.E. Vidale, F. Leyton, P. Shearer, *Inner-core fine-scale structure from scattered waves recorded by LASA*, J. Geophys. Res. 113, B09312 (2008).

[70] A. Piersanti, L. Boschi, A.M. Dziewonski, *Estimating lateral structure in the earth's outer core*, Geophys. Res. Lett., 28, 1659-1662 (2001).

[71] G. Poupinet, B.L.N. Kennett, *On the observation of high frequency PKiKP and its coda in Australia*, Phys. Earth Planet. Int. 146, 497511 (2004).

[72] B. Romanowicz, L. Bréger, *Anomalous splitting of free oscillations: A reevaluation of possible interpretations*, J. Geophys. Res. 105, 21559-21578 (2000).

[73] B. Romanowicz, H. Tkalčić, L. Bréger, *On the origin of complexity in PKP travel time data*, in *Core Dynamics, Structure and Rotation*, Dehant V et al. (eds.), pp. 3144, American Geophysical Union, Washington (2003).

[74] S. Rosat, *Time varying gravity in relation with the Earths intern dynamics: Contribution of superconducting gravimeters*, Doctoral Thesis, Strasbourg University, 2004.

[75] G. Roult, J. Roch, E. Clevede, *Observation of split modes from the 26th December 2004 Sumatra-Andaman megaevent*, Physics of the Earth and Planetary Interiors 179, 4559 (2010).

[76] P. Shearer, G. Masters, *The density and shear velocity contrast at the inner core boundary*, Geophys. J. Int. 102, 491-498 (1990).

[77] L.B. Slichter, *The fundamental free mode of the Earths inner core*, PNAS 47, 186190 (1961).

[78] G. Soldati, L. Boschi, A. Piersanti, *Outer core density heterogeneity and the discrepancy between PKP and PcP travel time observations*, Geophysical research letters 30, 1190 (2003).

[79] X. Song, P. G. Richards, *Seismological evidence for differential rotation of the Earthsinner core*, Nature 382, 221-224 (1996).

[80] A. Souriau, A. Teste, S. Chevrot, *Is there any structure inside the liquid outer core?*, Geophys. Res. Lett. 30, 1567 (2003).

[81] A. Souriau, *Deep Earth structure - the Earths cores*, in *Treatise on Geophysics*, Vol. 1, *Seismology and structure of the Earth*, edited by G. Schubert, B. Romanowicz, A. Dziewonski, 655-693, Elsevier, Amsterdam (2007).

[82] D.J. Stevenson, *Limits on lateral density and velocity variations in the earth's outer core*, Geophys. J. Roy. Astr. S. 88, 311-319 (1987).

[83] W. Su, A. M. Dziewonski, R. Jeanloz, *Planet within a planet: Rotation of the Inner Core of Earth*, Science 274, 1883-1887 (1996).

[84] I. Sumita, P. Olson, *A laboratory model for convection in Earths core driven by a thermally heterogeneous mantle*, Science, 286, 1547-1549 (1999).

[85] I. Sumita, P. Olson, *Rotating thermal convection experiments in a hemispherical shell with heterogeneous boundary heat flux: implications for the Earth's core*, J. Geophys. Res. 107, 2169 (2002).

[86] I. Sumita, M.I. Bergman, *Inner-Core Dynamics*, in *Treatise on Geophysics*, Vol. 8, *Core Dynamics*, edited by G. Schubert, P. Olson, 299-318, Elsevier, Amsterdam (2007).

[87] S. Tanaka and H. Hamaguchi, *Degree one heterogeneity and hemispherical variation of anisotropy in the inner core from PKP(BC)-PKP(DF) times*, J. Geophys. Res. 102, 2925-2938 (1997).

[88] H. Tkalčić, M. Young, T. Bodin, S. Ngo, M. Sambridge, *The shuffling rotation of the Earths inner core revealed by earthquake doublets*, Nature Geoscience 6, 497-502 (2013).

[89] C. Vamoş, N. Suciu, *Seismic hemispheric asymmetry induced by Earth's inner core decentering*, arXiv:1111.1121v1 [physics.geo-ph] (2011).

[90] E. Vesanen, R. Teisseyre, *Symmetry and asymmetry in geodynamics*, Geophysica 15, 147-170 (1978).

[91] J. Wahr, D. de Vries, *The possibility of lateral structure inside the core and its implications for nutation and earth tide observations*, Geophys. J. Int. 99, 511-519 (1989).

[92] L. Waszek, J. Irving, A. Deuss, *Reconciling the hemispherical structure of Earth's inner core with its superrotation*, Nature Geoscience 4, 264-267 (2011).

[93] L. Waszek, A. Deuss, *Distinct layering in the hemispherical seismic velocity structure of Earths upper inner core*, J. Geophys. Res. 116, B12313 (2011).

[94] L. Wen, F. Niu, *Seismic velocity and attenuation structures in the top of the Earth's inner core*, J. Geophys. Res. 107(B11), 2273 (2002).

[95] W. Yu, L. Wen, F. Niu, *Seismic velocity structure in the Earth's outer core*, J. Geophys. Res. 110, B02302 (2005).

[96] W. Yu, L. Wen, *Seismic velocity and attenuation structures in the top 400 km of the Earth's inner core along equatorial paths*, J. Geophys. Res. 111, B07308 (2006).

[97] D. Zidarov, *Theory of the evolution of the Earth and the Earth's crust based on the mobile Earth core concept*, Geol. Balcanica 7, 3-26 (1977).